Time-resolved photoluminescence of barium titanate ultrafine powders

S. G. Lu,[a] Z. K. Xu, and Haydn Chen
Department of Physics and Materials Science, City University of Hong Kong, 83 Tat Chee Avenue, Kowloon, Hong Kong

C. L. Mak and K. H. Wong
Department of Applied Physics and Materials Research Centre, The Hong Kong Polytechnic University, Hung Hom, Kowloon, Hong Kong

K. F. Li and K. W. Cheah
Department of Physics, Hong Kong Baptist University, Kowloon Tong, Kowloon, Hong Kong

(Received 28 March 2005; accepted 8 February 2006; published online 22 March 2006)

Time-resolved photoluminescence (PL) near 540 nm, taken from barium titanate ($BaTiO_3$) ultrafine powders of ~80, 90, and 110 nm in size, was measured at 11 K. Two-exponential functions were found to fit the decay curves well, and the decay lifetimes were composed of one short, about 10 ns, and one long, about 200 ns, time constants, respectively. Results also indicate that the PL peaks show a small blueshift with decreasing $BaTiO_3$ particle size. The decay process consists of the recombination of self-trapped excitons (long lifetime decay) and of the electrons in the surface states with the holes in the valence band (short lifetime decay). The short lifetime component makes comparable contribution to the decay intensity of PL with the long lifetime one. © *2006 American Institute of Physics*. [DOI: 10.1063/1.2182075]

I. INTRODUCTION

$BaTiO_3$ (BTO) is an incipient ferroelectric. It has been widely used in multilayer ceramic capacitors,[1] positive temperature coefficient thermistors,[2] and other electronic components. It can also be used as optical waveguide, as an alternative to $LiNbO_3$, or as optical devices by doping with rare-earth ions to take advantage of its electro-optical, photoluminescence, electroluminescence, and nonlinear optical properties.[3] With the miniaturization of electronic devices, ultrafine powders have been extensively investigated. Recently, ultrafine $BaTiO_3$ powders have been fabricated by sol-gel, hydrothermal, and other methods.[4–6]

The photoluminescence (PL) properties of $BaTiO_3$ ultrafine powders have been observed by several authors.[7–9] A model of self-trapped exciton (STE) was suggested to account for the observed phenomena. This model, however, has not been experimentally confirmed yet, especially in terms of the time-resolved PL spectrum. It is well known that STE has been found in alkali halides, condensed rare gases, organic molecular crystals, some oxides and other chalcogenides, a few semiconductor alloys, as well as quasi-one-dimensional materials.[10] STE has some common features. As conventional excitons, STE represents the interaction of electron and hole with the deformable lattice that produces a relaxed configuration of the pair. STE has some off-center structure and is related to the vacancies in the alkali halides. The recombination of the electron and hole is a transient process, and its decay usually consists of a fast process (short lifetime) and one or more slow processes (long lifetime). The transient absorption spectrum of STE has a "tail," called Urbach tail.[11] On the other hand, luminescences from bulk $BaTiO_3$ and $SrTiO_3$ crystals after irradiation at low temperature were ascribed to the presence of self-trapped excitons within TiO_6 octahedra,[12] viz., $Ti^{3+}-O^-$ STE. Therefore, it is worth studying the mechanism of PL in ultrafine powders and examining the relaxation process of STE by using time-resolved PL experiment. The time-resolved photoluminescence analysis is an effective method to address the excitation and recombination processes of electrons, holes, and excitons in the energy band gap of various semiconductors.[13–16] In this work, hydrothermal method was employed to prepare uniform BTO powders; the time-resolved photoluminescence was used to examine the luminescence process in the ultrafine BTO powders.

II. EXPERIMENTAL PROCEDURE

A. Sample preparation

Barium acetate $[Ba(CH_3COO)_2]$, tetrabutyl titanate $[Ti(OC_4H_9)_4]$, and tetramethyl-ammonium hydroxide (TMAH) were used as the starting materials, de-ionized water, and ethanol as the solvents. In this study, 5 mol % excess Ba^{2+} was added in order to avoid the formation of the Ti-rich phase in BTO. Barium acetate was firstly dissolved in de-ionized water. TMAH was then added slowly into the solution so as to let the final solution have a *p*H value over 13. After that, tetrabutyl titanate was added into the mixture and stirred for 10 min. The final precursor was poured into a Teflon cup inside the autoclave, and then the autoclave was placed in an oven and held at 120 °C for duration times of 3, 5, and 12 h, respectively. The Teflon vessel had a volume of 50 cm^3. The concentration of the $BaTiO_3$ precursor was fixed at 0.1–0.4*M*. After hydrothermal treatment, the supernatant solution was removed, and some acetic acid and boiled de-ionized water were added and stirred for about

[a]FAX: +852-2788-7052; electronic mail: apsglu@cityu.edu.hk

30 min. Then the mixture was filtered with a rotary pump. Finally the wet powders were dried in an oven at 120 °C for about 10 h.

B. PL measurement

For continuous wave (cw) PL measurements, the excitation source used was the 325 nm line of He–Cd laser (Kimmon IK5352R-D) with a maximum power of 4 mW. A circularly variable-metallic neutral-density attenuator was used to obtain a gradient intensity of excitation light. The excitation light was modulated at 730 Hz using a mechanical chopper (Standford SR540). The emitted light from the samples was collected by a 25 cm focal-length double monochromator (Oriel 77225) and detected by a thermoelectrically cooled photomultiplier tube (PMT) (Hamamatsu R636-10). A 345 nm filter was used to block the excitation light. A lock-in amplifier (Stanford SR830) system was used to record the PMT signal that had been amplified by a low noise current-to-voltage preamplifier (EG&G Instruments 5182). For low temperature measurement, the samples were mounted in a liquid helium closed-cycle cryostat (Oxford CC1104) pumped by a cryodriver (Edwards 1.5). The temperature inside the cryostat could be adjusted from 10 to 300 K using the temperature controller (Oxford IT502). For the lifetime measurement, the 337 nm line of the nitrogen laser (Laser Science, Inc. VSL-337ND-S) was used as the excitation light. The pulse width is 4 ns. The decay spectrum was monitored by an HP 600 MHz oscilloscope.

III. RESULTS AND DISCUSSION

A. Morphology and structure

Figure 1(a) shows a field emission scanning electron microscopy (FESEM) image of the BTO powders hydrothermally treated for 12 h. Ultrafine BTO powders are spherical, nonagglomerated, and have a uniform particle size of about 110 nm. It was found that the BTO particle size increased from 80 to 90 and 110 nm when the treatment duration increased from 3 to 5 and 12 h. These powders are referred to as BTO-01, BTO-02, and BTO-03 in the text, respectively. Figure 1(b) is a transmission electron microscopy image of BTO powders hydrothermally treated for 3 h, it further confirmed the spherical and nonagglomerated morphology of BTO particles.

Figure 2 shows the x-ray diffraction (XRD) patterns of BTO powders treated at 120 °C for 3, 5, and 12 h. Results indicate that all BTO powders are of pseudocubic perovskite structure. The peaks become sharper with increasing the duration time, but the peak positions are almost the same for three duration times. This means that the lattice constant of the BTO particles does not change with the duration time. The particle sizes D were calculated, according to Scherrer's equation, to be 80, 90, and 110 nm for the duration times of 3, 5, and 12 h, respectively.

B. Photoluminescence spectrum

Figure 3 illustrates the PL spectra, measured at 11 K, of BTO powders treated at 120 °C for different durations. The

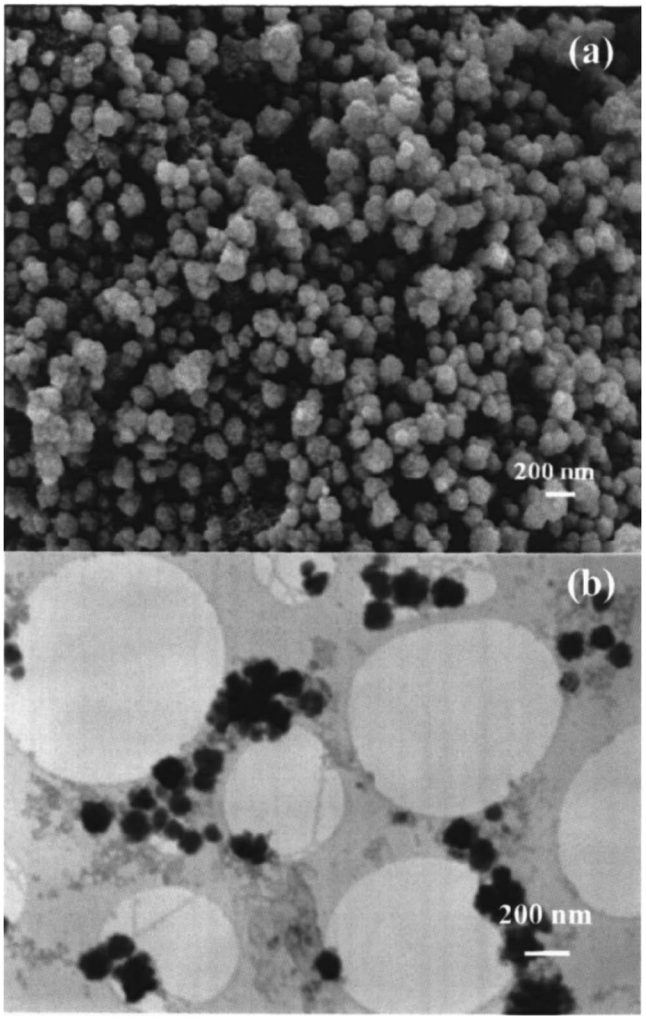

FIG. 1. (a) FESEM image of 110 nm $BaTiO_3$ ultrafine powders. (b) TEM image of 80 nm $BaTiO_3$ ultrafine powders.

PL spectrum of sample BTO-01 has a full width at half maximum (FWHM) of 0.49 eV, which was obtained by fitting the peak with a Gaussian distribution. Similarly, the PL peaks of samples BTO-02 and BTO-03 have the FWHMs of 0.43 and 0.41 eV, respectively. It was found that the PL peaks have a small shift (from 2.31 to 2.27 and 2.25 eV) with the variation of particle size (from 80 to 90 and 110 nm). The PL peak energy as a function of reciprocal of the square of the crystallite radius is shown in the inset (I). Since the energy band gap of bulk BTO is 2.9–3.4 eV, the luminescence states are obviously located within the energy band gap. It is known

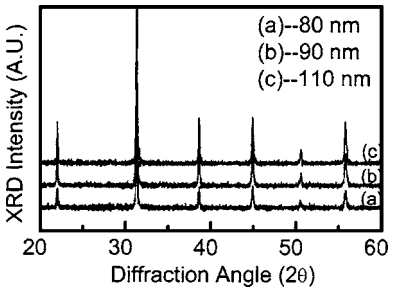

FIG. 2. XRD profiles of $BaTiO_3$ ultrafine powders. (a) 80, (b) 90, and (c) 110 nm.

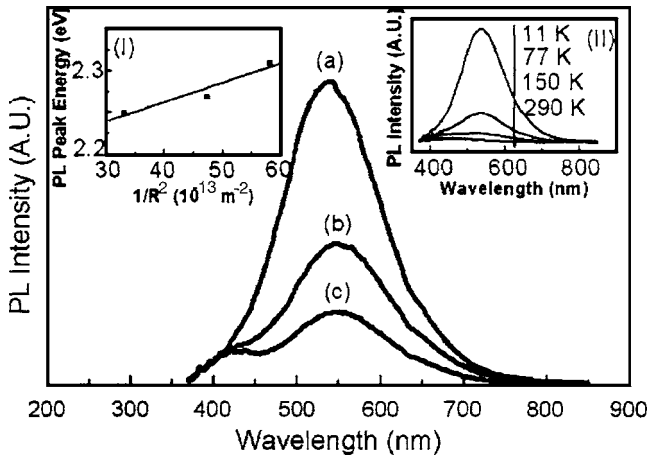

FIG. 3. Photoluminescence spectra of $BaTiO_3$ ultrafine powders. (a) 80, (b) 90, and (c) 110 nm. Inset (I) is the PL peak energy as a function of inverse square of the dimension and inset (II) is the PL intensities of sample (a) at temperatures from 11 to 290 K.

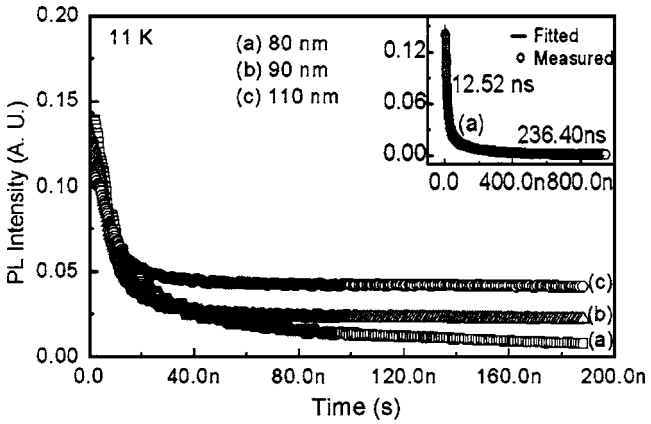

FIG. 4. Time-resolved photoluminescence of $BaTiO_3$ ultrafine powders. (a) 80, (b) 90, and (c) 110 nm. Inset is the fitting of the decay curve of sample (a).

that quantum size effect could shift the PL position in terms of either the band-to-band recombination or the recombination of electrons in the surface states with the holes in the valence band.[17] As observed in $(SrBa)Nb_2O_6$/silica nanocomposites,[18] ferroelectric nanoparticles (about 10 nm) also revealed the characteristics of quantum confinement. However, the BTO powders have particle sizes ranging from 80 to 110 nm, if there is any quantum size effect, it will be very weak. Because the lattice constants of three BTO powders are almost the same (see Fig. 1), it means that it is the surface states, resulted from the distorted crystalline structure, that determine the PL properties. Recently, Orhan *et al.*[19] investigated the room-temperature PL of $BaTiO_3$ powders based on experimental and theoretical study. They observed that only the structurally disordered samples exhibit the PL properties at room temperature. The first-principle calculation indicated that the crystalline BTO presents a higher band gap than the disordered BTO, and charge transfer occurs from $[TiO_5]$ cluster to the $[TiO_6]$ one, revealing the intrinsic presence of trapped holes and electrons, and Jahn-Teller bipolarons, in the disordered BTO powders. Although the particles of BTO powders obtained by hydrothermal treatment are crystalline, the surface of the particles is distorted, even disordered. The PL, however, mainly reflects the surface properties. Therefore, the surface states play a critical role in determining the PL characteristics. Because all the surface states in three BTO powders are distorted lattice or defects, the distortions or defects are random; therefore, the PL peak occurs at a similar wavelength. Nevertheless, the PL is the recombination of STE and the recombination between the electrons in the surface states and the holes in the valence band; the particle size has an impact on the PL peak position since it affects the valence band energy or energy band gap. Moreover, dielectric confinement effects will simultaneously act on the ultrafine BTO powders in terms of the self-trapped excitons.[20]

C. Time-resolved PL spectrum

The decay curves of PL of three BTO powders are sketched in Fig. 4. The curves can be fitted by the following formula;[21]

$$I(t) = \sum_{i=1} A_i e^{-t/\tau_i}, \tag{1}$$

where I is the PL intensity and A_i and τ_i are the preexponential factor and the time constant of the ith lifetime. Their integrated intensities at the peak can be written as[21]

$$P(t) = \int_t^\infty I(t)dt = \sum_i A_i \tau_i e^{-t/\tau_i}, \tag{2}$$

where P is the integrated PL intensity and $A_i\tau_i$ is the intensity coefficient of the ith lifetime.

Table I summarizes the values of τ_i, A_i, and $A_i\tau_i$ for three BTO powders. In the table, A_i and $A_i\tau_i$ are normalized such that $I(0)=1$ and $P(t)=1$. During the fitting, using two exponentials seemed to be sufficient to fit the data. This means that there are two decay processes taking place in the PL transition here, one is short, about 10 ns, and the other is longer, about 200 ns. For the peak intensity, about 90% is associated with the short lifetime component. This feature is consistent with that of STE in alkali halides where big differences are also demonstrated. Here, firstly, the longer lifetimes are smaller than those in the alkali halides by three

TABLE I. Parameters in Eqs. (1) and (2) by fitting the decay curves.

Temperature		11 K		77 K	
BTO-01	τ_i	12.52 ns	236.40 ns	9.96 ns	132.81 ns
	A_i	89.5%	10.5%	90.84%	9.16%
	$A_i\tau_i$	31.10%	68.90%	42.65%	57.35%
BTO-02	τ_i	8.71 ns	167.60 ns	8.22 ns	218.49 ns
	A_i	95.15%	4.85%	95.97%	4.03%
	$A_i\tau_i$	50.47%	49.53%	47.24%	52.76%
BTO-03	τ_i	9.23 ns	186.91 ns	7.99 ns	219.16 ns
	A_i	95.42%	4.58%	97.01%	2.99%
	$A_i\tau_i$	50.73%	49.27%	54.21%	45.79%

orders of magnitude; secondly, for the $A_i\tau_i$ coefficient, the short lifetime component at 11 K increases from 31.10% for BTO-01 to 50.47% and 50.73% for BTO-02 and BTO-03, respectively. This means that the short lifetime component makes almost the same contribution to the emission intensity as the long lifetime one. With increasing particle size, the contribution of short lifetime component to the emission intensity increases, correspondingly the contribution of long lifetime component decreases. This is different from the STE in alkali halides where the long lifetime component is dominant. The distinction may be attributed to the influence of the size effect. We may assume that the long lifetime emission comes from STEs which are composed of bound excitons, the recombination of electrons in the surface states to the holes in valence band, while the short lifetime emission comes from the electrons in the lower energy surface states recombining with the holes in the valence band. In both cases, the decrease of particle size may result in the blueshift of emission peak. The temperature dependence of the PL reveals that STEs in the BTO ultrafine powders are related to the bound excitons which are formed by vacancies or lattice distortion,[10] indicated by the fact that the excitons mainly behave at low temperature but quench at about 150 K. As temperature rises to room temperature, the bound excitons will convert into free excitons, then the population of the bound excitons will be very small, so the recombination rate is also very low; thus the PL intensity becomes rather weak. Inset (II) of Fig. 3 is the PL versus temperature for sample (a) (80 nm, treated at 120 °C for 3 h). Other samples exhibited similar results. The fact that perovskite structure containing titanium-oxygen octahedra shows similar photoluminescence at visible wavelength suggests that PL is mainly related to the oxygen octahedron. The distortion of the oxygen octahedron on the surface of the ultrafine powder may lead to the enhancement of the PL intensity due to the decrease of Ti–O distance.[22] Therefore the recombination of self-trapped exciton and of electrons in the surface states with holes in the valence band in the ultrafine powders may exhibit a higher PL intensity and a higher quench temperature, (even at room temperature[8,9]) when the particle size further decreases. As mentioned in Sec. I, the phenomenon has been observed by other authors.[7–9]

IV. CONCLUSIONS

Ultrafine barium titanate powders were prepared by a hydrothermal process. Time-resolved photoluminescence experiment was conducted. Results indicated that the PL peaks reveal blueshift characteristics with decreasing BTO particle size. The decay curves of PL have similar characteristics as those obtained in alkali halides. The short lifetime PL component makes comparable contribution to the decay intensity of PL with long lifetime component, and this contribution decreases with the decreasing particle size.

ACKNOWLEDGMENTS

The work was supported by a RGC CERG grant (No. CityU 1049/02) and a NSFC/RGC grant (Project No. 9050172) at the City University of Hong Kong, and a grant (G-T473) at The Hong Kong Polytechnic University.

[1] P. Ward, *Electronic Ceramics*, edited by B. C. H. Steele (Elsevier, New York, 1991), p. 29.
[2] W. Heywang and H. Thomann, *Electronic Ceramics*, edited by B. C. H. Steele (Elsevier, New York, 1991), p. 49.
[3] B. A. Block and B. W. Wessels, Appl. Phys. Lett. **65**, 25 (1994).
[4] M. H. Frey and D. A. Payne, Phys. Rev. B **54**, 3158 (1996).
[5] S. O'Brien, L. Brus, and C. B. Murray, J. Am. Chem. Soc. **123**, 12085 (2001).
[6] B. Grohe, G. Miehe, and G. Megner, J. Mater. Res. **16**, 1901 (2001).
[7] J. F. Meng, Y. B. Huang, W. F. Zhang, Z. L. Du, Z. Q. Zhu, and G. T. Zou, Phys. Lett. A **205**, 72 (1995).
[8] M. S. Zhang, Z. Yin, Q. Chen, W. F. Zhang, and W. C. Chen, Solid State Commun. **119**, 659 (2001).
[9] J. Yu, J. L. Sun, J. H. Chu, and D. Y. Tang, Appl. Phys. Lett. **77**, 2807 (2000).
[10] K. S. Song and R. T. Williams, *Self-trapped Excitons*, Springer Series in Solid-State Sciences Vol. 105 (Springer-Verlag, Berlin, 1993).
[11] M. Schreiber and Y. Toyozawa, J. Phys. Soc. Jpn. **52**, 318 (1983).
[12] M. Aguilar and F. Agullo-Lopez, J. Appl. Phys. **53**, 9009 (1982).
[13] G. Schlegel, J. Bohnenberger, I. Potapova, and A. Mews, Phys. Rev. Lett. **88**, 137401 (2002).
[14] K. B. Nam, J. Li, M. L. Nakarmi, J. Y. Lin, and H. X. Jiang, Proc. SPIE **4992**, 202 (2003).
[15] S. W. Jung, W. I. Park, H. D. Cheong, G. C. Yi, H. M. Jang, S. Hong, and T. Joo, Appl. Phys. Lett. **80**, 1924 (2002).
[16] Y. Zhang, M. D. Sturge, K. Kash, B. P. Van der Gaag, A. S. Gozdz, L. T. Florez, and J. P. Harbison, J. Lumin. **60/61**, 400 (1994).
[17] L. E. Brus, J. Chem. Phys. **80**, 4403 (1984).
[18] S. G. Lu, C. L. Mak, K. H. Wong, and K. W. Cheah, Appl. Phys. Lett. **79**, 4310 (2001).
[19] E. Orhan *et al.*, Phys. Rev. B **71**, 085113 (2005).
[20] J. Yu, J. L. Sun, J. H. Chu, and D. Y. Tang, Appl. Phys. Lett. **77**, 2807 (2000).
[21] R. T. Williams, M. N. Kabler, W. Hayes, and J. P. Stott, Phys. Rev. B **14**, 725 (1976).
[22] B. Bouma and G. Blasse, J. Phys. Chem. Solids **56**, 261 (1995).